MATHEMATICAL MODELING AND COMPUTING, Vol. 12, No. 1, pp. 187–196 (2025)

Mixed convection of nanofluid at the lower stagnation point of a horizontal circular cylinder: Brinkman–viscoelastic

Fauzi F.[1,2], Kasim A. R. M.[1], Kanafiah S. F. H. M.[2]

[1] *Centre for Mathematical Sciences, University Malaysia Pahang Al-Sultan Abdullah (UMPSA), 26300 Gambang, Pahang, Malaysia*
[2] *College of Computing, Informatics and Mathematics, University Teknologi MARA (UiTM) Kelantan Branch, 18500 Machang, Kelantan, Malaysia*

(Received 15 October 2024; Revised 17 February 2025; Accepted 18 February 2025)

Researchers have formulated the Brinkman–viscoelastic model to study the convective heat transfer of viscoelastic fluids traversing porous media recently. Nevertheless, they did not employ nanofluids. Currently, scientists and researchers are employing nanofluids and hybrid nanofluids in their studies, products, and technologies due to their ability to enhance the transfer of heat. Therefore, the aim of this research is to study the heat transfer of a viscoelastic fluid with nanoparticles as it moves over a horizontal circular cylinder in a saturated porous region at the lower stagnation point. The model, described by a collection of partial differential equations, is simplified into solvable equations by utilizing non-dimensional and non-similarity variables. The simplified system of equations is then solved using the Runge–Kutta–Fehlberg technique and the outcomes are verified through comparative study. It has been found that the temperature goes up when the Brinkman parameter, the viscoelastic parameter, and the volume fraction of nanoparticles are all raised. This temperature rise indicates convective heat transfer.

Keywords: *viscoelastic; nanofluid; porous media; Brinkman.*
2010 MSC: 34B09, 76D05, 76A05 **DOI:** 10.23939/mmc2025.01.187

1. Introduction

Convective heat transfer refers to the process of transferring thermal energy between a surface and a fluid as a result of the fluid's movement. It is a common occurrence in various engineering and industrial processes. Convective heat transfer involves two types of fluids: Newtonian and non-Newtonian. However, these fluids are not as efficient as metals when it comes to heat transfer. To address this issue, the thermal conductivity of the fluid can be enhanced by incorporating nanoparticles into the fluid [1]. Choi and Eastman introduced the term "nanofluid" in 1995, and subsequent research at the Argonne National Laboratory established the concept of nanofluid [2]. Nanofluids have demonstrated a thermal conductivity twice as high as traditional fluids. As a result, nanofluids have been suggested to exceed the performance of heat transfer of fluids [3].

Convective heat transfer in porous mediums has numerous thermal engineering applications, including fiber and granular insulation and geophysical thermal and insulation engineering. Mathematicians engage in the theoretical study of heat transmission in porous medium by developing and solving mathematical models. There are many research have been conducted to study the flow of fluid and nanofluid through porous medium. Reference [4] is a study that built upon the research conducted by [5] on porous medium. They replaced the ordinary fluid with nanofluid, analyzed the flow and specifically focused on the impact of nanoparticles on the natural convection occurring past a vertical plate, utilising Buongiorno's model. There are several mathematical models have been developed and

This work was supported by grant FRGS/1/2023/STG06/UMP/02/7 Ministry of Higher Education Malaysia.

mainly used in studying and describing flow of fluid through porous medium. The Brinkman model is one of those mathematical models. A combination of models also has been developed to analyze heat transfer of fluids with varying properties. The work [6] combined the Brinkman model as used in [7] and viscoelastic model as mentioned in [8], resulting in Brinkman–Viscoelastic model to analyze convective heat transfer of viscoelastic fluid flowing through porous medium.

Regarding nanofluids, there exist multiple models for studying the convective heat transfer of nanofluids. Notably, the Tiwari and Das and Buongiorno models are widely recognized in this field. The Tiwari and Das model analyses the nanofluid's behavior by taking into account the nanofluid's solid volume fraction. For this research, the Tiwari and Das model is employed which has demonstrated successful application in numerous studies [9–14].

As previously noted, nanofluid has a better capacity to transfer heat, therefore this study complements the work [15] by changing the conventional viscoelastic fluid with viscoelastic nanofluid. All in all, the main goal of this study is to combine the Tiwari and Das model and Brinkman–Viscoelastic model and use this new combined model to examine mixed convective heat transfer at lower stagnation point of viscoelastic fluid containing nanoparticles flowing over a horizontal circular cylinder that is saturated in a porous region. Since this study concentrates on a horizontal circular cylinder, the stagnation point is where the vertical flow first hits the bottom of the cylinder.

2. Mathematical formulation

Referring to the advancement of Brinkman model when including nanofluids investigated by [16] from their previous work in 2003 [7] and research by [2] and [17], there will be some changes in momentum and energy equations. The parameters in the governing equations represent the characteristics of nanofluids, namely μ_{nf}, $(\rho C_p)_{nf}$ and α_{nf} representing dynamic viscosity, heat capacitance and thermal diffusivity of nanofluid respectively. Let the horizontal circular cylinder that is embedded in porous medium has radius a. It is assumed that it is independent of the nanoparticle size and nanoparticle is introduced in mass/volume fraction. T_w and T_∞ are used to represent the constant temperature of the cylinder surface and constant ambient respectively. $\bar{u}_e(\bar{x}) = U_\infty \sin(\bar{x}/a)$ is the external flow's velocity and the coordinate $\bar{x}$ represents the measurement from lower stagnation point along the surface of the cylinder [18]. The free stream velocity denoted by $\frac{1}{2}U_\infty$ is directed in the vertical upward direction relative to the cylinder, while the symbol g represents the acceleration of gravity.

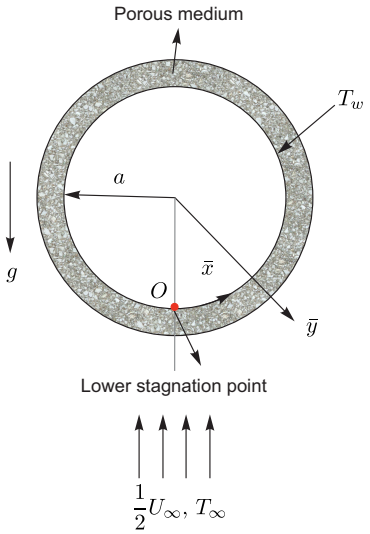

Fig. 1. The problem's coordinate system and model.

Figure 1 depicts the problem's physical model along with the coordinate system. Given that the study is centered at the lower stagnation point, variables $\bar{x}$ and $\bar{y}$ are assigned specific values. In particular, $\bar{x}$ is set to 0, while $\bar{y}$ is chosen to be perpendicular to the surface of the cylinder. Based on the specified assumptions and the boundary layer approximation, the nanofluid parameters utilized by [16] and [2] are incorporated into the fundamental governing equations of the Brinkman–viscoelastic model proposed by [15], resulting in the governing equations for this study,

$$\frac{\partial \bar{u}}{\partial \bar{x}} + \frac{\partial \bar{u}}{\partial \bar{y}} = 0, \tag{1}$$

$$\frac{\mu_{nf}}{K}\bar{u} = \frac{\mu_{nf}}{\phi}\frac{\partial^2 \bar{u}}{\partial \bar{y}^2} + \bar{u}_e\frac{\partial \bar{u}_e}{\partial \bar{x}} + k_0\left[\bar{u}\frac{\partial^3 \bar{u}}{\partial \bar{x}\partial \bar{y}^2} + \bar{v}\frac{\partial^3 \bar{u}}{\partial \bar{y}^3} - \frac{\partial \bar{u}}{\partial \bar{y}}\frac{\partial^2 \bar{u}}{\partial \bar{x}\partial \bar{y}} + \frac{\partial \bar{u}}{\partial \bar{x}}\frac{\partial^2 \bar{u}}{\partial \bar{y}^2}\right] + \left[\varphi\rho_s\beta_s + (1-\varphi)\rho_f\beta_f\right]g(T - T_\infty)\sin(\bar{x}/a), \tag{2}$$

$$(\rho C_p)_{nf}\left(\bar{u}\frac{\partial T}{\partial \bar{x}} + \bar{v}\frac{\partial T}{\partial \bar{y}}\right) = k_{nf}\left(\frac{\partial^2 T}{\partial \bar{x}^2} + \frac{\partial^2 T}{\partial \bar{y}^2}\right). \tag{3}$$

Equations (1)–(3) represent the continuity, momentum, and energy equations of the study, respectively, subject to the Constant Wall Temperature (CWT) boundary condition

$$\begin{aligned} &\bar{u}=0, \quad \bar{v}=0, \quad T=T_w \quad \text{on} \quad \bar{y}=0, \\ &\bar{u}\to\bar{u}_e, \quad T\to T_\infty \quad \text{as} \quad \bar{y}\to 0. \end{aligned} \tag{4}$$

Here T is the fluid temperature, $\bar{p}$ is the fluid pressure, φ is the volume fraction of nanoparticle, μ_f is the viscosity of the fluid fraction, β_s and β_f are the thermal expansion coefficients of the solid and of the fluid, respectively, ρ_s is the density of the solid fraction and ρ_f is the density of the fluid fraction. The relations between nanofluid and conventional fluid are given by [2, 16]

$$\begin{aligned} &\mu_{nf}=\frac{\mu_f}{(1-\varphi)^{2.5}}, \quad \alpha_{nf}=\frac{k_{nf}}{(\rho C_p)_{nf}}, \quad (\rho C_p)_{nf}=(1-\varphi)(\rho C_p)_f+\varphi(\rho C_p)_s, \\ &\frac{k_{nf}}{k_f}=\frac{(k_s+2k_f)-2\varphi(k_f-k_s)}{(k_s+2k_f)+\varphi(k_f-k_s)}. \end{aligned} \tag{5}$$

The variables in the equations are defined as follows: k_{nf} represents the nanofluid's effective thermal conductivity, k_f represents the fluid's thermal conductivity, k_s represents the solid's thermal conductivity, $(\rho C_p)_{nf}$ represents the nanofluid's heat capacity, $(\rho C_p)_f$ represents the fluid's heat capacity and $(\rho C_p)_s$ represents the solid's heat capacity [19]. Carboxymethyl Cellulose (CMC) is a viscoelastic fluid, and [20] assessed its application as the base fluid in a microchannel heat sink (MCHS), revealing that it possesses a perfect heat transfer ratio. Copper is a nanoparticle with excellent thermal conductivity, along with others such as Arabic Gum (Ag) and Aluminium (Al) [21]. The base fluid utilised in this study is Carboxymethyl Cellulose (CMC) water, and the nanoparticle employed is Copper (Cu). Table 1 shows the thermophysical properties of these two materials [2].

Table 1. Base fluid and nanoparticle thermophysical properties [22].

Physical properties	Density (kg/m^3)	Heat capacity (J/kg·K)	Thermal conductivity (W/mK)	Coefficients of thermal expansion (1/k)
Base fluid (CMC)	$\rho_f=997.1$	$(\rho C_p)_f=4179$	$k_f=0.613$	$\beta_f=21$
Nanoparticle (Cu)	$\rho_s=8933$	$(\rho C_p)_s=385$	$k_s=400$	$\beta_s=1.67$

To solve the nonlinear equations (1)–(4), reducing them to non-dimensional form by incorporating non-dimensional variables followed by similarity transformation to simplify the equations into less complex partial differential equations is necessary. The employed non-dimensional variables are defined as [19, 23]:

$$\begin{aligned} &x=\bar{x}/a, \quad y=\mathrm{Pe}^{1/2}(\bar{y}/a), \quad u=\bar{u}/U_\infty, \quad v=\mathrm{Pe}^{1/2}(\bar{v}/U_\infty), \\ &\theta=(T-T_\infty)/(T_w-T_\infty), \quad u_e(\bar{x})=\bar{u}_e(\bar{x})/U_\infty, \quad p=(\bar{p}-p_\infty)/\left(\rho_{nf}U_\infty^2\right) \end{aligned} \tag{6}$$

with porous medium modified Peclet number $\mathrm{Pe}=U_\infty a/\alpha_m$. Substituting (6) into (1)–(4), the following boundary layer equations are obtained:

$$\frac{\partial u}{\partial x}+\frac{\partial v}{\partial y}=0, \tag{7}$$

$$\begin{aligned} \frac{1}{(1-\varphi)^{2.5}}\frac{\partial u}{\partial y}&=\frac{\Gamma}{(1-\varphi)^{2.5}}\frac{\partial^3 u}{\partial y^3} \\ &+k_1\left[\frac{\partial u}{\partial y}\frac{\partial^3 u}{\partial x\partial y^2}+u\frac{\partial^4 u}{\partial x\partial y^3}+\frac{\partial v}{\partial y}\frac{\partial^3 u}{\partial y^3}+v\frac{\partial^4 u}{\partial y^4}-\frac{\partial^2 u}{\partial y^2}\frac{\partial^2 u}{\partial x\partial y}-\frac{\partial u}{\partial y}\frac{\partial^3 u}{\partial x\partial y^2}+\frac{\partial^2 u}{\partial y\partial x}\frac{\partial^2 u}{\partial y^2}+\frac{\partial u}{\partial x}\frac{\partial^3 u}{\partial y^3}\right] \\ &+\left[(1-\varphi)+\varphi(\rho_s\beta_s/\rho_f\beta_f)\right]\lambda\frac{\partial\theta}{\partial y}\sin x, \end{aligned} \tag{8}$$

$$u\frac{\partial\theta}{\partial x}+v\frac{\partial\theta}{\partial y}=\frac{\alpha_{nf}}{\alpha_f}\frac{\partial^2\theta}{\partial y^2}, \tag{9}$$

$$\begin{aligned} u = 0, \quad v = 0, \quad \theta = 1 \quad \text{at} \quad \bar{y} = 0, \\ u \to u_e, \quad v \to 0, \quad \theta \to 0 \quad \text{as} \quad \bar{y} \to \infty. \end{aligned} \tag{10}$$

Upon obtaining the non-dimensional form of the equations, the similarity transformation variables defined below are employed to convert the equations into solvable equations,

$$\psi = x\, f(x, y), \quad \theta = \theta(x, y), \tag{11}$$

with ψ represents the function of stream while θ represents the fluid's temperature and both are defined as $u = \frac{\partial \psi}{\partial y}$ and $v = -\frac{\partial \psi}{\partial x}$. The transformed and solvable system of equations is shown below,

$$\begin{aligned} \frac{f'}{(1-\varphi)^{2.5}} = \frac{\Gamma f'''}{(1-\varphi)^{2.5}} + k_1\left[2f'f''' - f\, f^{(4)} - (f'')^2\right] + \left[(1-\varphi) + \varphi\left(\rho_s\beta_s/\rho_f\beta_f\right)\right]\lambda\,\theta\,\frac{\sin x}{x} \\ + \frac{\sin x}{x\,(1-\varphi)^{2.5}} + k_1 x\left[f'\frac{\partial f'''}{\partial x} - \frac{\partial f}{\partial x}f^{(4)} + \frac{\partial f'}{\partial x}f''' - f''\frac{\partial f''}{\partial x}\right], \end{aligned} \tag{12}$$

$$\frac{k_{nf}}{k_f}\left[\frac{(\rho\, C_p)_f}{(1-\varphi)(\rho\, C_p)_f + \varphi(\rho\, C_p)_s}\right]\theta'' + f\,\theta' = x\left[f'\frac{\partial \theta}{\partial x} - \frac{\partial f}{\partial x}\theta'\right], \tag{13}$$

$$\begin{aligned} f(x,0) = 0, \quad f'(x,0) = 0, \quad \theta(x,0) = 1 \quad \text{at} \quad y = 0, \\ f'(x,\infty) \to \frac{\sin x}{x}, \quad f''(x,\infty) \to 0, \quad \theta(x,\infty) \to 0 \quad \text{as} \quad y \to \infty. \end{aligned} \tag{14}$$

At the lower stagnation point, the value of x is 0, allowing (12) to (14) to be expressed in a simplified form of differential equations as demonstrated below,

$$\frac{f'}{(1-\varphi)^{2.5}} - \frac{\Gamma f'''}{(1-\varphi)^{2.5}} - k_1\left[2f'f''' - f f^{(4)} - (f'')^2\right] - \left[(1-\varphi) + \varphi(\rho_s\beta_s/\rho_f\beta_f)\right]\lambda\,\theta - \frac{1}{(1-\varphi)^{2.5}} = 0, \tag{15}$$

$$\frac{k_{nf}}{k_f}\left[\frac{(\rho\, C_p)_f}{(1-\varphi)(\rho\, C_p)_f + \varphi(\rho\, C_p)_s}\right]\theta'' + f\,\theta' = 0 \tag{16}$$

with the boundary condition

$$\begin{aligned} f(0) = 0, \quad f'(0) = 0, \quad \theta(0) = 1, \\ f'(\infty) \to 1, \quad f''(\infty) \to 0, \quad \theta(\infty) \to 0. \end{aligned} \tag{17}$$

The primes represent derivatives relative to y, with $\Gamma = \frac{\mathrm{Da}}{\phi}\mathrm{Pe}$ [6], $\phi = \frac{\mu_f}{\tilde{\mu}}$ [2], $\lambda = \frac{\mathrm{Ra}}{\mathrm{Pe}}$ [19] and $k_1 = \frac{k_0 K U_\infty \mathrm{Pe}}{\mu a^3}$ [6] being Brinkman, porosity, mixed convection and viscoelastic parameters, respectively and $\mathrm{Da} = \frac{K}{a^2}$ [6] and $\mathrm{Ra} = \frac{g\,K\beta(T_w - T_\infty)a}{\alpha_m \nu}$ [15] being Darcy and Rayleigh numbers respectively, and $\tilde{\mu}$ is the effective dynamic viscosity.

The skin friction coefficient C_f is a crucial dimensionless parameter that characterizes the behaviour of the convective boundary layer, representing the shear stress at the surface resulting from viscous forces when a fluid flows over it. It is defined as follows [2]:

$$C_f = \frac{\tau_w}{\rho\, U_\infty^2}, \tag{18}$$

where $\tau_w = \mu_{nf}\left(\frac{\partial \bar{u}}{\partial \bar{x}}\right) + k_0\left(\bar{u}\frac{\partial^2 \bar{u}}{\partial \bar{x}\partial \bar{y}} + \bar{v}\frac{\partial^2 \bar{u}}{\partial \bar{y}^2} + 2\frac{\partial \bar{u}}{\partial \bar{x}}\frac{\partial \bar{u}}{\partial \bar{y}}\right)$ is the wall shear stress [2]. After conducting non-dimensional and non-similarity transformations using (6) and (11), the skin friction (18) turns into

$$C_f = \frac{1}{(1-\varphi)^{2.5}}\frac{\mathrm{Pr}}{\mathrm{Pe}^{1/2}}\, x\, f'', \tag{19}$$

where Pe and Pr are Peclect number and Prandtl number respectively.

3. Results

The simplified equations (15), (16) and (17) are then numerically solved using the Runge–Kutta–Fehlberg method, which has its built-in program in the Maple software. The solution are solved for several values of mixed convection λ, Brinkman Γ, viscoelastic k_1 parameters and nanoparticle volume fraction φ. For generating asymptote boundary conditions, the boundary layer thickness for this study is set within the range of 8 units. The simulations utilize a fixed parameter of mixed convection, with a value of $\lambda = 1$ for assisting flow, unless otherwise specified. In order to validate the findings, the results of this study are compared with the results documented and published in [7] and [15] as shown in Table 2. From the table, it can be seen that there is a lot of agreement in the result that validates the suggested calculation correctness.

Table 2. Comparison for values of $f''(0)$ and $-\theta'(0)$ with $\Gamma = 0.1$, $k_1 = 0$, $\varphi \to 0$ and several value of $\lambda = 0.5, 1, 2, 3$.

λ	$f''(0)$ [7]	$-\theta'(0)$ [7]	f"(0) [15]	$-\theta'(0)$ [15]	$f''(0)$ This study	$-\theta'(0)$ This study
0.5	4.3999	0.7240	4.3999	0.7239	–	–
1	5.5923	0.7791	5.5922	0.7790	5.5923	0.7790
2	7.8768	0.8706	7.8767	0.8705	7.8768	0.8705
3	10.1613	0.9460	10.1612	0.9458	10.0613	0.9458

Figure 2 illustrates the variations in temperature and fluid velocity profiles as the value of Brinkman parameter Γ is altered. The value of Γ varies from a range of 0.2 to 2.0, as indicated by the research conducted by [17]. From Figure 2*a*, it is identified that the velocity decreases as the Brinkman parameter Γ increases, this phenomenon may be attributed to the enhancement of drag force resulting from the relative velocity between the horizontal circular cylinder and the fluid. As the Brinkman parameter increases, there is an increase in the temperature growth as shown in Figure 2*b*.

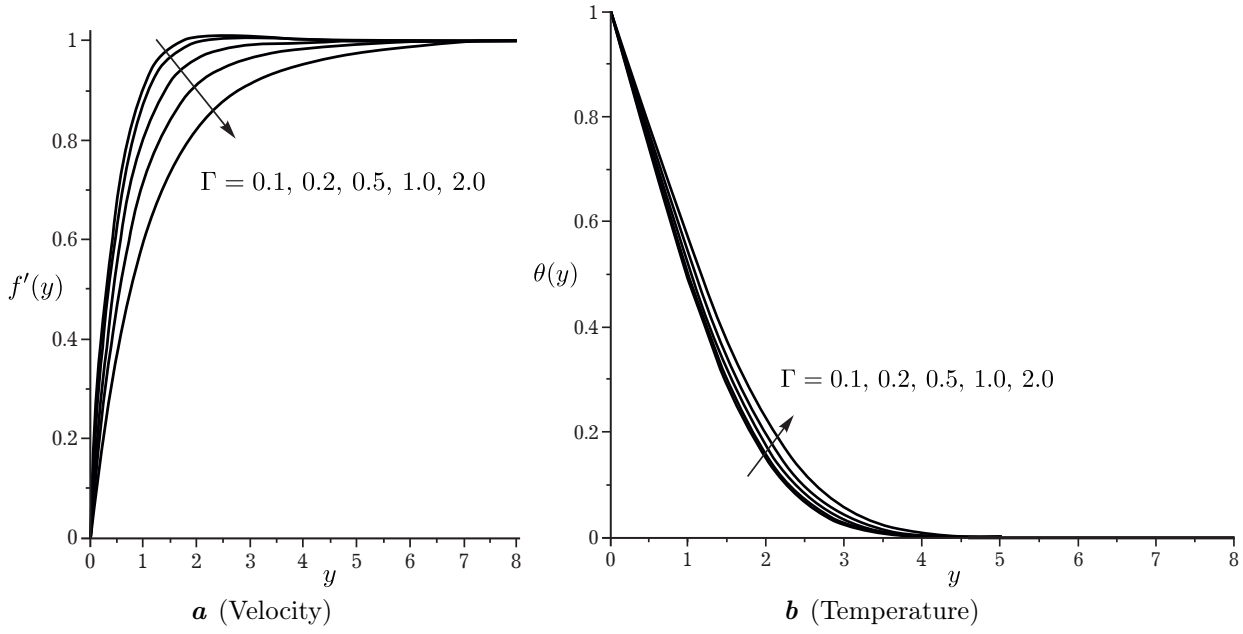

a (Velocity) ***b*** (Temperature)

Fig. 2. Impact of Brinkman parameter Γ.

Further, the value of $f''(0)$ and $\theta(0)$ are calculated and presented in Table 3 for $k_1 = 0.01$ and several values of λ and φ as used in [15]. The results of [15] for the Brinkman–viscoelastic fluid model were also included in this table. It can be seen that when the value of φ is set to be 0, the outcomes for the Brinkman–viscoelastic nanofluid model are identical to the Brinkman–viscoelastic fluid model.

Table 3. Values of $f''(0)$ and $-\theta'(0)$ for $\varphi = 0, 0.01, 0.02, 0.03, 0.04$ and various value of λ.

λ	$f''(0)$ [15]	$-\theta'(0)$ [15]	$f''(0)$ $\varphi = 0$	$f''(0)$ $\varphi = 0.02$	$f''(0)$ $\varphi = 0.04$	$-\theta'(0)$ $\varphi = 0$	$-\theta'(0)$ $\varphi = 0.02$	$-\theta'(0)$ $\varphi = 0.04$
0.1	3.1752	0.6623	3.1752	3.0394	2.9054	0.6623	0.6283	0.5957
0.2	3.3972	0.6747	3.3927	3.2500	3.1086	0.6747	0.6403	0.6072
0.3	3.6068	0.6866	3.6068	3.4570	3.3090	0.6866	0.6518	0.6183
0.4	3.8175	0.6980	3.8175	3.6616	3.5066	0.6980	0.6628	0.6290
0.5	4.0252	0.7089	4.0252	3.8630	3.7016	0.7089	0.6734	0.6393
0.6	4.2300	0.7195	4.2300	4.0617	3.8940	0.7195	0.6837	0.6492
0.7	4.4317	0.7297	4.4317	4.2578	4.0841	0.7297	0.6936	0.6587
0.8	4.6310	0.7396	4.6310	4.4514	4.2718	0.7396	0.7031	0.6680
0.9	4.8276	0.7491	4.8276	4.6426	4.4573	0.7491	0.7124	0.6770
1	5.0218	0.7583	5.0218	4.8315	4.6408	0.7583	0.7213	0.6857

Figure 3 shows the impact of the viscoelastic k_1 parameter on the temperature and velocity of the fluid. The values of k_1 vary from a range of 0.5 to 3.5, as indicated in [17]. Referring to Figure 3a, as the value of k_1 increases, the velocity of the fluid drops. It demonstrates that the speed decreases when there is an increment in viscosity. While for temperature, it exhibits an inverse correlation with the increase in the value k_1 as shown in Figure 3b. This phenomenon arises from the fluid's viscosity and elasticity properties.

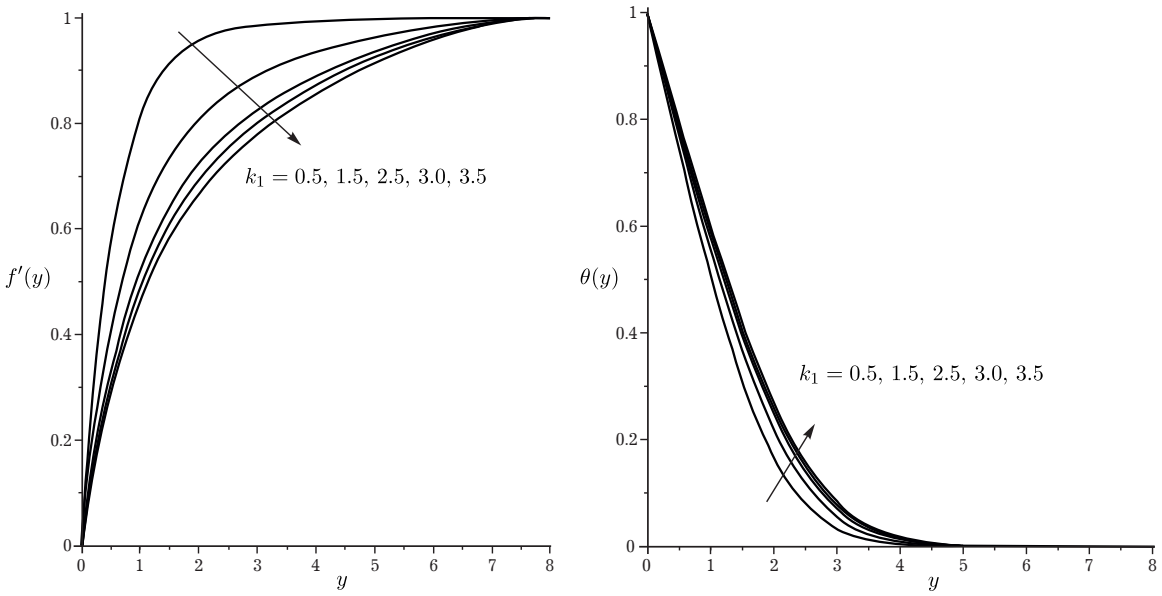

a (Velocity) ***b*** (Temperature)

Fig. 3. Impact of viscoelastic parameter k_1.

Figure 4 illustrates the relationship between different mixed parameter values λ in velocity and temperature. The value of λ varies from a range of 1 to 4, as indicated in [17]. It can be seen that the velocity increases as the parameter λ increases Figure 4a. It has been determined that the velocity exceeds the expected limits for high λ values. Divergent patterns have been noted in the temperature profile where the convective heat transfer decreases as the value of λ increases resulting in a fall in temperature as shown in Figure 4b.

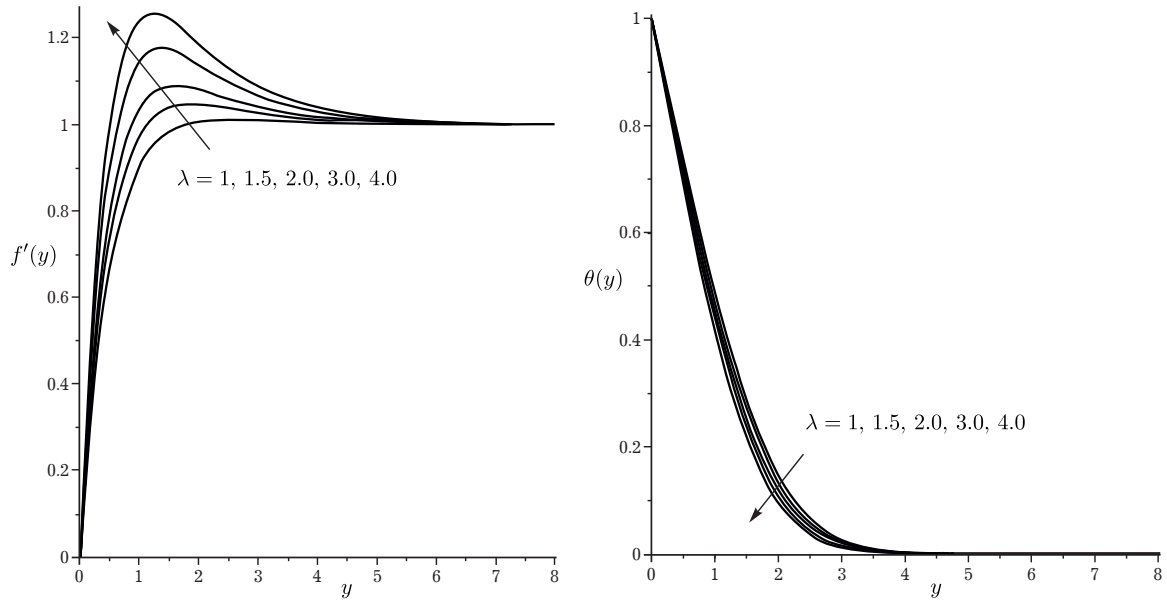

a (Velocity) ***b*** (Temperature)

Fig. 4. Impact of mixed parameter λ.

Figure 5 illustrates the velocity and temperature patterns for varying nanoparticle volume fraction φ. The value of φ varies from the range 0 to 0.4, as indicated in [2]. Both velocity and temperature profiles exhibit an increasing trend as the value of φ increases from 0 to 0.04. The rise in temperature may be attributed to the thermal conductivity of the nanofluid.

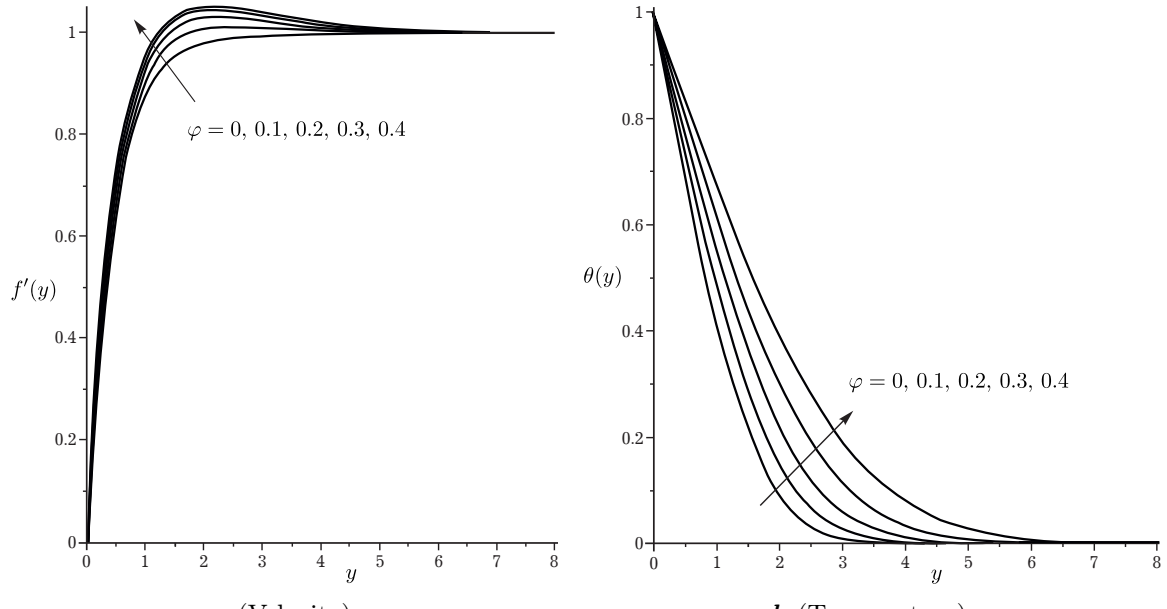

a (Velocity) ***b*** (Temperature)

Fig. 5. Impact of nanoparticle volume fraction φ.

Figure 6 illustrates the velocity profile of Brinkman viscoelastic fluid and Brinkman viscoelastic nanofluid under $\lambda = 1$, $\lambda = 0.1$ and $k_1 = 0.3$. The velocity profile of Brinkman viscoelastic nanofluid with a value of $\varphi = 0.2$ (dash line) is greater than that of Brinkman viscoelastic fluid (full line).

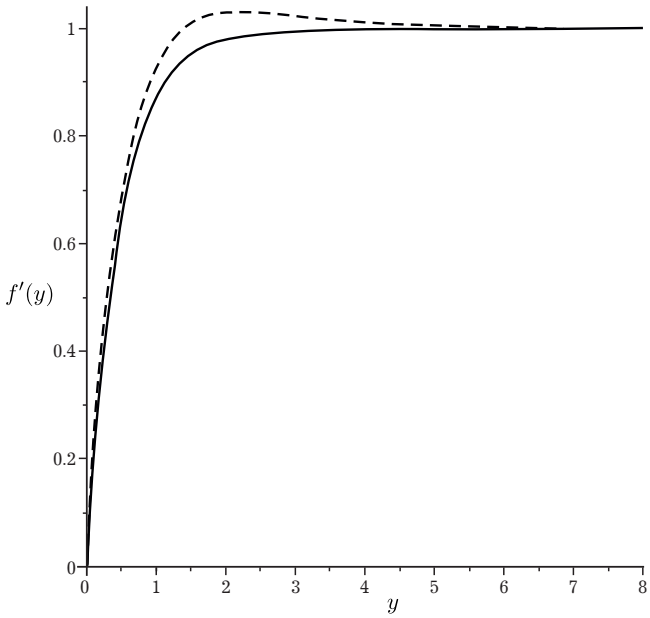

Fig. 6. Velocity of Brinkman viscoelastic fluid vs Brinkman viscoelastic nanofluid.

This study examines the skin friction at the lower stagnation point, when $x = 0$, resulting in a C_f of zero at that point. Skin friction arises from the tangential movement of fluid particles across a surface and is directly correlated with the shear stress resulting from the velocity gradient close to the surface. At the stagnation point, the fluid velocity relative to the surface is zero, as the flow stop entirely at that location. Because of that, the shear stress and skin friction are likewise zero.

4. Conclusion

This research investigates the issue of mixed convection boundary layer flow around a horizontally oriented cylinder, concentrating on the lower stagnation point with a constant wall temperature within a porous medium saturated by a viscoelastic nanofluid, utilising the Brinkman–viscoelastic model and the Tiwari and Das nanofluid model. The analysis examines the impacts of the Brinkman parameter, mixed parameter, viscoelastic parameter, and nanoparticle volume fraction on the velocity $f'(y)$ and temperature $\theta(y)$, which can be summarized as follows:

1. An increase in the value of Brinkman and viscoelastic parameters resulted in a reduction of velocity.
2. An augmentation in the fraction of nanoparticle volume and mixed convective parameter led to an enhancement in velocity.
3. An increase in the value of Brinkman parameter, viscoelastic parameter and nanoparticle volume fraction resulted in an increase in temperature.

This study, concentrating on the mixed convection heat transfer at the lower stagnation point, may provide a foundation for subsequent investigations into the flow dynamics surrounding a horizontal circular cylinder from that point.

Acknowledgement

The authors express gratitude to the Ministry of Higher Education Malaysia for financial assistance through the Fundamental Research Grant Scheme (FRGS), FRGS/1/2023/STG06/UMP/02/7 (University reference RDU230124), and the Tabung Persidangan Dalam Negara (TPDN) from University Malaysia Pahang Al-Sultan Abdullah. Gratitude is also extended to University Technology Mara Kelantan Campus, Machang Branch for their encouragement and support.

[1] Tiwari R. K., Das M. K. Heat transfer augmentation in a two-sided lid-driven differentially heated square cavity utilizing nanofluids. International Journal of Heat and Mass Transfer. **50** (9–10), 2002–2018 (2007).

[2] Mahat R., Rawi N. A., Kasim A. R. M., Shafie S. Mixed convection flow of viscoelastic nanofluid past a horizontal circular cylinder with viscous dissipation. Sains Malaysiana. **47** (7), 1617–1623 (2018).

[3] Khashi'ie N. S., Waini I., Zokri S. M., Kasim A. R. M., Arifin N. M., Pop I. Stagnation point flow of a second-grade hybrid nanofluid induced by a Riga plate. International Journal of Numerical Methods for Heat & Fluid Flow. **32** (7), 2221–2239 (2022).

[4] Kuznetsov A. V., Nield D. A. Thermal instability in a porous medium layer saturated by a nanofluid: Brinkman model. Transport in Porous Media. **81**, 409–422 (2010).

[5] Cheng P., Minkowycz W. J. Free convection about a vertical flat plate embedded in a porous medium with application to heat transfer from a dike. Journal of Geophysical Research. **82** (14), 2040–2044 (1977).

[6] Kanafiah S. F. H. M., Kasim A. R. M., Zokri S. M., Arifin N. S. Non-similarity solutions of non-Newtonian Brinkman-viscoelastic fluid. Mathematics. **10** (12), 2023 (2022).

[7] Nazar R., Amin N., Pop I. Mixed convection boundary layer flow from a horizontal circular cylinder in micropolar fluids: case of constant wall temperature. International Journal of Numerical Methods for Heat & Fluid Flow. **13** (1), 86–109 (2003).

[8] Anwar I., Amin N., Pop I. Mixed convection boundary layer flow of a viscoelastic fluid over a horizontal circular cylinder. International Journal of Nin-Linear Mechanics. **43** (9), 814–821 (2008).

[9] Mohamed M. K. A., Salleh M. Z., Jamil F. C., Ruey O. H. Free convection boundary layer flow over a horizontal circular cylinder in Al_2O_3-Ag/Water hybrid nanofluid with viscous dissipation. Malaysian Journal of Fundamental and Applied Sciences. **17** (1), 20–25 (2021).

[10] Mohamed M. K. A., Ishak A., Pop I., Mohammad N. F., Soid S. K. Free convection boundary layer flow from a vertical truncated cone in a hybrid nanofluid. Malaysian Journal of Fundamental and Applied Sciences. **18**, 257–270 (2022).

[11] El-Zahar E. R., Rashad A. M., Saad W., Seddek L. F. Magneto-hybrid nanofluids flow via mixed convection past a radiative circular cylinder. Scientific Reports. **10** (1), 10494 (2020).

[12] Yasin S. H. M., Mohamed M. K. A., Ismail Z., Salleh M. Z. MHD Free convection boundary layer flow near the lower stagnation point flow of a horizontal circular cylinder in ferrofluid. IOP Conference Series: Materials Science and Engineering. **736**, 022117 (2020).

[13] Afsana S., Nag P., Molla M. M., Thohura S. Natural convection flow of nanofluids over horizontal circular cylinder with uniform surface heat flux. AIP Conference Proceedings. **2324**, 050024 (2021).

[14] Elfiano E., Ibrahim N. M. I. N., Mohamed M. K. A. Mixed convection boundary layer flow over a horizontal circular Cylinder Al_2O_3-Ag/water hybrid nanofluid with viscous dissipation. CFD Letters. **16** (4), 98–110 (2024).

[15] Kanafiah S. F. H. M., Kasim A. R. M., Zokri S. M., Arifin N. S. Numerical investigation at lower stagnation point flow over a horizontal circular cylinder of Brinkman-viscoelastic fluid. Journal of Advanced Research in Fluid Mechanics and Thermal Sciences. **87** (2), 56–65 (2021).

[16] Nazar R., Tham L., Pop I., Ingham D. B. Mixed convection boundary layer flow from a horizontal circular cylinder embedded in a porous medium filled with a nanofluid. Transport in Porous Media. **86** (2), 517–836 (2011).

[17] Kanafiah S. F. H. M., Kasim A. R. M., Zokri S. M., Arifin N. S., Manaf Z. I. A. Flow analysis of Brinkman-viscoelastic fluid in boundary layer region of horizontal circular cylinder. CFD Letters. **14** (12), 27–37 (2022).

[18] Merkin J. H. Mixed convection from a horizontal circular cylinder. International Journal of Heat and Mass Transfer. **20** (1), 73–77 (1977).

[19] Tham L., Nazar R., Pop I. Mixed convection boundary layer flow past a horizontal circular cylinder embedded in a porous medium saturated by a nanofluid: Brinkman model. Journal of Porous Media. **16** (5), 445–457 (2013).

[20] Al-Rashed A. A. A. A., Shahsavar A., Entezari S., Moghimi M. A., Adio S. A., Nguyen T. K. Numerical investigation of non-Newtonian water-CMC/CuO nanofluid flow in an offset strip-fin microchannel heat sink: Thermal performance and thermodynamic considerations. Applied Thermal Engineering. **155**, 247–258 (2019).

[21] Konkwo E. C., Osho I. W., Almanassra I. W., Abdullatif Y. M., Al-Ansari T. An updated review of nanofuids in various heat transfer devices. Journal of Thermal Analysis and Calorimetry. **145**, 2817–2872 (2021).

[22] Zokri S. M., Salleh M. Z., Kasim A. R. M., Arifin N. S. Lower stagnation point flow of convectively heated horizontal circular cylinder in Jeffrey nanofluid with suction/injection. Journal of Advanced Research in Fluid Mechanics and Thermal Sciences. **76** (1), 135–144 (2020).

[23] Kanafiah S. F. H. M., Kasim A. R. M., Zokri S. M., Shafie S. Numerical solutions of convective transport on Brinkman-viscoelastic fluid over a bluff body saturated in porous region. Case Studies in Thermal Engineering. **28**, 101341 (2021).

Змішана конвекція нанофлюїду в нижній точці застою горизонтального круглого циліндра: в'язкопружна модель Брінкмана

Фаузі Ф.[1,2], Касім А. Р. М.[1], Канафія С. Ф. Х. М.[2]

[1]*Центр математичних наук,*
Університет Малайзії Паханг Аль-Султан Абдулла (UMPSA),
26300 Гамбанг, Паханг, Малайзія
[2]*Коледж обчислювальної техніки, інформатики та математики,*
Університет Технології MARA (UiTM), Келантанський філіал,
18500 Мачанг, Келантан, Малайзія

Дослідники нещодавно сформулювали в'язкопружну модель Брінкман для вивчення конвективного теплообміну в'язкопружних рідин, що проходять через пористі середовища. Проте вони не використовували нанофлюїди. Наразі вчені та дослідники використовують нанофлюїди та гібридні нанофлюїди у своїх дослідженнях, продуктах і технологіях завдяки їхній здатності покращувати передачу тепла. Тому метою даного дослідження є дослідження теплообміну в'язкопружної рідини з наночастинками під час її руху по горизонтальному круглому циліндру в насиченій пористій області в нижній точці застою. Модель, описану набором диференціальних рівнянь у частинних похідних, спрощено до розв'язуваних рівнянь за допомогою безвимірних і неподібних змінних. Потім спрощену систему рівнянь розв'язують за допомогою техніки Рунге–Кутта–Фельберга, а результати перевіряють шляхом порівняльного дослідження. Було встановлено, що температура зростає, коли параметр Брінкмана, параметр в'язкопружності та об'ємна частка наночастинок підвищуються. Це підвищення температури свідчить про конвективний теплообмін.

Ключові слова: *в'язкопружний; нанофлюїд; пористі середовища; Брінкман.*